

Fabrication of High Aspect Ratio Ferroelectric Microtubes by Vacuum Infiltration using Macroporous Silicon Templates

S. S. N. Bharadwaja,[†] M. Olszta, and S. Trolier-McKinstry

Materials Research Institute, The Pennsylvania State University, University Park, Pennsylvania 16802

X. Li and T. S. Mayer

Electrical Engineering Department, The Pennsylvania State University, University Park, Pennsylvania 16802

F. Roozeboom

Philips Research Laboratories, Eindhoven, the Netherlands

Ordered arrays of high aspect ratio (>10:1) ferroelectric $\text{Pb}(\text{Zr}_{0.52}\text{Ti}_{0.48})\text{O}_3$ (PZT) tube structures were fabricated by vacuum infiltration of macroporous silicon (Si) templates. Improved phase purity was achieved when PZT microtubes were pyrolyzed at 300°C and partially released from the Si template to prevent a chemical reaction between the Pb and the Si during subsequent high-temperature crystallization. The free-standing microtubes were crystallized by rapid thermal annealing at 750°C for 1–3 min. Perovskite phase formation was confirmed by X-ray diffraction and transmission electron microscopy methods. Coaxial structures comprised of metallic LaNiO_3 , PZT, and Pd layers were also processed to enable future electrical characterization of the ferroelectric microtubes.

I. Introduction

THE ability to make piezoelectric devices with complex designed structures enables one to tailor stress and electric field profiles to optimize response.^{1–3} While fabrication techniques for such solid pillar structures are available for milli- to micrometer-scale devices,^{4,5} the processing of micrometer-scale piezoelectric tube arrays is less well described in the literature. This paper details the processing of 1–3 microtube air/piezoelectric composites with large aspect ratios (length to diameter >10). Arrays of high aspect ratio piezoelectric structures are anticipated to offer advantages in a variety of piezoelectric sensors and actuators,⁶ high-resolution biomedical ultrasound systems, and tunable photonic applications.⁷

In addition to device applications, such free-standing microtubes offer the opportunity to study the properties of piezoelectric thin films without the influence of substrate clamping. Most thin films are under hundreds of MPa to GPa of in-plane stress as a consequence of intrinsic growth stresses, lattice misfits in unrelaxed films, and/or the thermal expansion coefficient mismatch between the film and the substrate. These stresses can shift the transition temperature, alter the equilibrium domain structure, change the order of the phase transition, affect the domain wall mobility, and shift the phase transition sequence as a function of temperature.^{8–11} Eliminating the substrate should greatly reduce such effects¹² and allow investigations of the role of substrate clamping on factors such as the mobility of domain walls.

Current manufacturing methods to process high aspect ratio structures at the micrometer scale can be classified into (1) top-down, (2) bottom-up, and (3) template replication routes. In the

top-down approach, precise structures can be processed using conventional lithography, combined with microfabrication techniques. $\text{Pb}(\text{Zr}_{0.52}\text{Ti}_{0.48})\text{O}_3$ (PZT) nanostructures have been prepared using electron beam and focused ion beam techniques.^{13,14} However, the walls of these structures were exposed to high-energy ion bombardment during processing that could induce crystallographic damage or non-stoichiometry. In the bottom-up approach, many synthesis schemes have been reported for processing ferroelectric structures. Recently, Suyal *et al.*¹⁵ and Liu *et al.*¹⁶ reported processing of KNbO_3 nanorods using a hydrothermal process. Urban *et al.*¹⁷ reported processing of single crystalline BaTiO_3 nanowires using the decomposition of a barium titanium isopropoxide ($\text{BaTi}[\text{OCH}(\text{CH}_3)_2]_6$) precursor. The major disadvantage of this approach is the random positioning of the particles created.

The third technique involves replicating the pores of microporous and mesoporous templates such as polymer resists, Si, or anodized alumina to form high aspect ratio ferroelectric tubes or rods. The advantage of this synthetic route is that well-aligned and ordered multicomponent oxide structures can be processed. Aoki *et al.*¹⁸ reported fabrication of $(\text{Pb},\text{La})(\text{Zr},\text{Ti})\text{O}_3$ pillars 0.6–2 μm in lateral dimension and up to 1 μm tall using a sol-gel infiltration of an e-beam patterned photoresist. Fabrication of ferroelectric nanotubes utilizing anodized alumina and anodized titania membranes has also been reported.¹⁹ Mishina *et al.*²⁰ and Luo *et al.*²¹ molded ferroelectric microtubes by infiltrating the pores of Si templates with PZT solution under room-temperature and pressure conditions. Recently, Morrison *et al.*²² reported processing of bismuth layer structure ferroelectric microtubes by liquid source-misted chemical deposition using Si templates.

Chemical reactions between the ferroelectric and the template walls, especially at high temperatures, can lead to the formation of secondary phases that play a crucial role in determining the final properties of these structures. In particular, many samples prepared in Si templates showed some residual amorphous phase.^{19,20} This paper outlines a process for optimizing phase purity in crystalline and ordered arrays of high aspect ratio ferroelectric PZT microtubes using vacuum infiltration of Si templates. In addition, the processing of potential electrodes, including LaNiO_3 and Pd, as well as coaxial multilayer tube structures, such as $\text{LaNiO}_3/\text{PZT}/\text{LaNiO}_3/\text{Pd}$, is described.

II. Experimental Procedure

(1) Materials

Macroporous Si templates (Philips Research Laboratories, Eindhoven, the Netherlands, or Norcada Inc., Edmonton, Canada) consisting of hexagonal two-dimensional (2D) pore arrays were created by deep reactive ion etching (DRIE). These tem-

M. Kuwabara—contributing editor

plates have pore diameters and an inter-pore separation of 1.8–2.0 and 1.5 μm , respectively.

Chemical solution deposition was used to prepare all of the microtube structures described in this paper. A 2-methoxyethanol-based 0.70–0.75M PZT solution was used to process the PZT microtubes. The precursors used to prepare the PZT solution were lead acetate trihydrate (99.99%), zirconium (IV) propoxide (99.999%), titanium (IV) isopropoxide (99.999%), and 2-methoxyethanol (+99.9%). Details of the PZT solution processing are given elsewhere.²³ A 0.3M LaNiO_3 solution was prepared by mixing a stoichiometric ratio of lanthanum nitrate hexahydrate (99.99%) and nickel (II) acetate tetrahydrate (99.99%) in 2-methoxyethanol and refluxing at 105°–110°C for 3 h. The Pd solution was prepared by mixing poly (D,L-lactide) and palladium (III) acetate (+99.9%) in a 1:1 ratio. These were then dissolved in chloroform (99.8% A.C.S. spectrophotometric grade).²⁴ All the chemicals were purchased from Sigma-Aldrich (St. Louis, MO).

(2) Template Cleaning

Before infiltrating the chemical solutions, the templates were cleaned to eliminate moisture, and layers of organics and silicon dioxide (SiO_2) present on the sidewalls of the pores. For this, the templates were first exposed to an oxygen plasma operated at 100 mTorr with an RF power of 80 W for 10 min (Plasma Technology Inc, Concord, MA) to remove any hydrocarbon polymer residue that passivates the pore sidewall during Si DRIE. Subsequently, the templates were immersed with a 10:1 buffered oxide etch (BOE) solution (from J. T. Baker) for 10 min. to remove the SiO_2 and expose a bare Si surface. A slight vacuum was drawn over the surface of the BOE solution to remove gas trapped in the pores and facilitate uniform infiltration of the etchant. After this step, the templates were taken out of the BOE solution and rinsed thoroughly with deionized water. Water infiltration into the pores was achieved via vacuum infiltration.

(3) Processing Technique and Characterization

Figure 1 shows a flow chart of the processing steps for making high aspect ratio tube structures. Cleaned and dried Si templates were immersed in a sealed container of PZT solution. The pressure above the solution was reduced to approximately 20 kPa below atmospheric pressure using a dry vacuum pump to facilitate uniform infiltration of the solution into the pores. This minimized the entrapment of air in the pores that otherwise led to incomplete infiltration (see Fig. 2).

Bubbling of the solution because of removal of the trapped gas in the Si pores was observed during vacuum infiltration, and completion of the infiltration was identified by termination of bubble formation in the PZT solution. This typically took about 5 min per infiltration. Such bubble formation was not observed when the above process was repeated with an unpatterned Pt-coated silicon substrate. After each infiltration, the surface of the template was cleaned using a cotton swab dipped in 2-methoxyethanol to remove the excess solution from the surface of the template. The samples were then pyrolyzed at 300°–350°C for 1 min in air. This process was repeated several times to build up the PZT layer in the templates to the desired wall thickness. Typically, a 300 nm PZT wall thickness was achieved in 17 infiltrations.

After PZT infiltration, the microtubes were partially released from the silicon matrix using one of two methods:

(i) *Wet chemical etch*: The PZT layer was first heat treated in a rapid thermal annealer in O_2 for 2 min to crystallize it. For release, a 30 wt% KOH in a water solution maintained at 70°C was used as an etch solution. Templates with crystallized PZT tubes were immersed in the etchant until the tubes were released from the surface. The released tubes were rinsed thoroughly with deionized water several times.

(ii) *Reactive ion etching*: A brief plasma etch in $\text{CF}_4\text{:O}_2$ was used to remove any residual gel as well as the native SiO_2 layer from the top surface of the Si template. An isotropic-pulsed

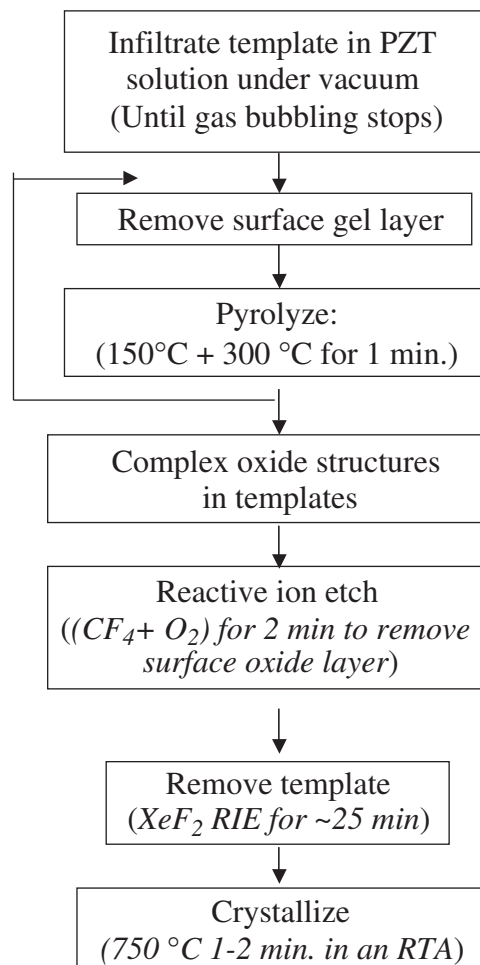


Fig. 1. Flow chart for fabricating $\text{Pb}(\text{Zr}_{0.52}\text{Ti}_{0.48})\text{O}_3$ (PZT) microtubes by vacuum infiltration of chemical solutions into the pores of a Si template.

XeF_2 RIE operated at a pressure of 1 Torr with a pulse cycle of 1 min was used to partially release the tubes (Xetch e'; series, Xactix Inc., Pittsburgh, PA). In most cases, $\sim 27 \mu\text{m}$ of Si was removed to produce an ordered array of free-standing PZT microtubes anchored at the bottom. The samples were heat treated in 99.98% oxygen using a rapid thermal annealer to examine

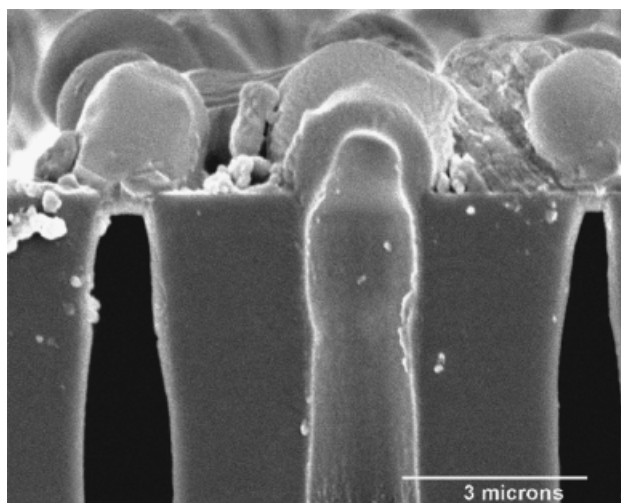


Fig. 2. Scanning electron microscope photograph of dome-shaped $\text{Pb}(\text{Zr}_{0.52}\text{Ti}_{0.48})\text{O}_3$ (PZT) caps on the silicon pores formed during infiltration of PZT at atmospheric pressure. Incomplete and non-uniform infiltration resulted during this process.

perovskite phase formation as a function of the annealing temperature.

Similar infiltration procedures were used to process LaNiO_3 and Pd microtubes to optimize the processing conditions individually. The surface of the Si template was cleaned after each infiltration using cotton swabs dipped in 2-methoxyethanol (LaNiO_3 solutions) and/or chloroform (for Pd solution) to avoid blocking the pores. Pyrolysis of LaNiO_3 layers in the silicon template was performed at 150°C for 2 min, followed by 300°C for 2 min. These tubes were crystallized in oxygen at temperatures between 600° and 750°C for 1–2 min using a rapid thermal annealer (RTA). LaNiO_3 was typically crystallized within the Si template to enable subsequent infiltrations (e.g., with PZT). For the Pd microtubes, a three-step solvent removal/pyrolysis process was used: 100°C for 5 min, followed by 250°C for 10 min, and finally at 400°C for 5 min. The Pd structures were crystallized at 550° – 700°C for 1–2 min in a nitrogen ambient using an RTA. In the case of Pd tubes, the residual Pd gel layer on the surface of the template was removed using an Ar ion beam etch after the crystallization.

Coaxial microtube structures consisting of $\text{LaNiO}_3/\text{PZT}/\text{LaNiO}_3/\text{Pd}$ layers were also fabricated using vacuum infiltration to enable outer and inner electrical contacts to the ferroelectric PZT tubes. LaNiO_3 (pseudo cubic perovskite structure with a lattice parameter ~ 0.386 nm) was chosen as an outer shell layer because it is conductive and can be used to integrate Pb-based ferroelectric thin layers directly on silicon substrates.^{25,26} The use of this layer thus enables each of the materials to be crystallized individually while still in the Si template, which facilitates building concentric electrode/ferroelectric/electrode structures. In this case, the Si templates were first infiltrated with a 2-methoxyethanol-based 0.3M LaNiO_3 solution following similar processing steps as those for PZT. The LaNiO_3 structures were pyrolyzed at 350° – 400°C for 5 min, followed by the heat treatments mentioned above. The PZT solution was subsequently infiltrated using the same procedure and heat treatments mentioned above. After crystallization of the PZT (lattice parameter ~ 0.408 nm), another layer of LaNiO_3 was processed in the same manner. After this, an inner Pd layer was prepared. This layer can act as an etch stop during patterning of the contacts for electrical measurements. After completing build up of the co-axial multilayer microtube structures inside the silicon molds, the template surface was cleaned using an argon ion-milling step, followed by RIE and XeF_2 etching as detailed earlier.

The surface morphology of the microtubes was examined using scanning electron microscopy (SEM; Model: Hitachi S-3500 N, Pleasanton, CA). For tube wall thickness measurements, a field emission SEM (Model: JEOL 6700F, Peabody, MA) was used. Crystallization was confirmed via X-ray diffraction (XRD; Scintag, Sunnyvale, CA) using $\text{CuK}\alpha$ radiation for 2θ from 20° to 65° with a 0.025° step size and a 60 s exposure time/step. The samples were examined using a Philips 420 TEM (Briarcliff Manor, NY) at an accelerating voltage of 120 keV. To prepare TEM samples, ~ 180 nm thick tubes were initially dispersed in ethanol and subsequently a drop of the solution was placed on a lacy carbon grid.

III. Results and Discussion

Using the method of vacuum infiltration in silicon templates, ordered arrays of ferroelectric structures could be achieved by annealing partially released structures at elevated temperatures as shown in Fig. 3. It was found that the use of KOH to release the PZT microtubes led to pitted sidewalls, probably because of chemical attack of the PZT by the strong base. To eliminate this type of damage, samples were released using a XeF_2 gas phase removal of the Si.

Vacuum infiltration allowed the chemical solutions to deposit evenly at the bottom of the Si template pores. Figure 4 shows SEM images of PZT and Pd microtubes that were released from the template by RIE and sonication. It is clear that the bases of the tubes are closed. In order to characterize the uniformity of

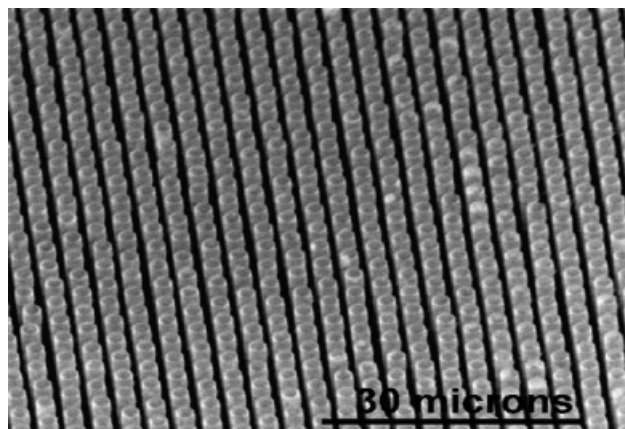


Fig. 3. Scanning electron microscope photograph of an ordered array of $\text{Pb}(\text{Zr}_{0.52}\text{Ti}_{0.48})\text{O}_3$ microtubes.

the tubes produced by vacuum infiltration, the wall thickness was measured along the length of the tube. This was done by partially releasing samples, and then breaking off the projecting tubes to expose the cross section. Controlled released depths were achieved by removing ~ 1 μm of Si per XeF_2 gas pulse. The layer thickness was measured by field emission SEM. Figure 5 shows the uniformity in the wall thickness of PZT, LaNiO_3 , and Pd tubes along the tube length. It can be seen that along the majority of the length, the tube walls produced are nearly constant in cross section. The thickness at the base is difficult to measure by this technique. Optical microscopy suggests that there is an increase in wall thickness near the closed end of the tube. From the wall thickness measurements, the estimated layer thickness for PZT, LaNiO_3 , and Pd tubes per infiltration was 18.1 ± 0.6 nm, 10 nm, and 20 nm, respectively.

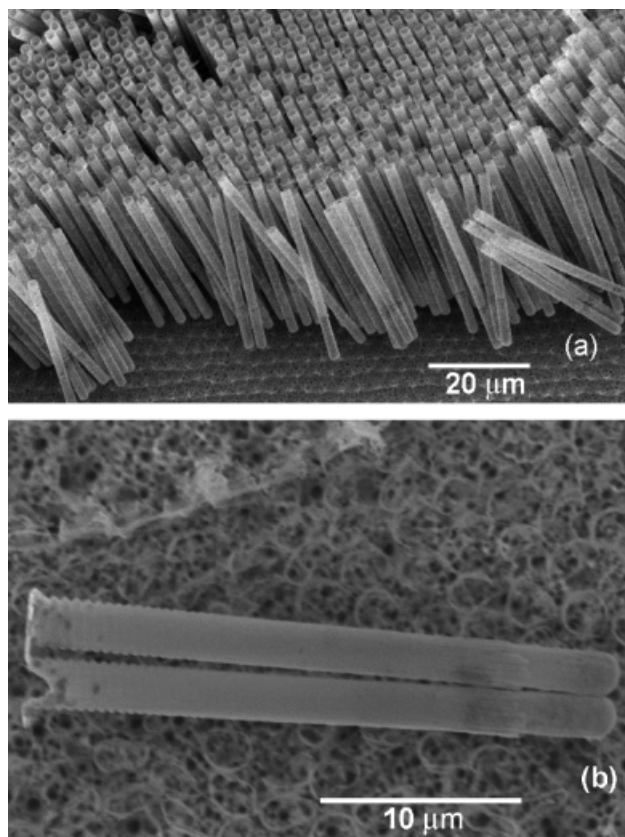


Fig. 4. Scanning electron microscope images of released (a) $\text{Pb}(\text{Zr}_{0.52}\text{Ti}_{0.48})\text{O}_3$ and (b) Pd microtubes. The closed ends of the tubes confirm infiltration of solution along the pore length using vacuum infiltration. The rippled sidewalls replicate the original pore geometry.

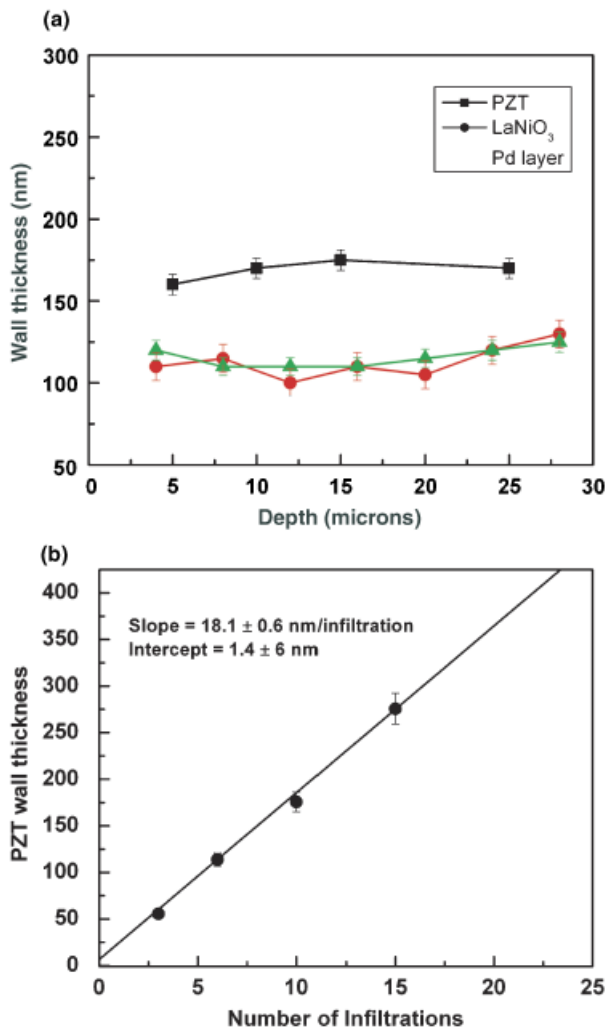


Fig. 5. (a) Uniformity of wall thickness as a function of depth for tubes produced using the vacuum infiltration method. (b) $\text{Pb}(\text{Zr}_{0.52}\text{Ti}_{0.48})\text{O}_3$ (PZT) tube wall thickness as a function of the number of infiltrations.

Figure 6 shows a cross-sectional SEM image of a PZT/Pd concentric bi-layer structure. For this purpose, 150 nm thick PZT and 100 nm thick Pd layers were processed using the vacuum infiltration method. For cross-sectional SEM images, the samples were prepared as mentioned above. As can be seen, the inner Pd layer has large grains compared with the inner PZT layer. Progressive sectioning of the infiltrated tubes shows the same features all along the tube length. Thus, well-defined co-axial structures were achieved. The use of inner and outer electrodes in tube structures should enable much lower driving voltages than can be achieved for structures electroded on the tube ends. In addition, the higher achievable capacitance should be very useful for electrical impedance matching.

XRD patterns of PZT and LaNiO₃ tubes annealed at various temperatures are shown in Fig. 7. The LaNiO₃ tubes were crystallized in the silicon molds before release. Crystallization occurred between 600° and 675°C in LaNiO₃ tube structures. Complete perovskite phase formation was achieved at 750°C in an RTA for 1 min in an oxygen ambient. The PZT tubes were released from the Si template along the majority of their length to minimize reaction with the Si before annealing them at various temperatures. As has typically been reported for the processing of planar films, on heat treatment, a pyrochlore or fluorite phase develops first.²⁷ Perovskite peaks appeared in PZT tubes at 700°C. The pyrochlore phase was detected in PZT tubes annealed below 750°C. As the thermal budget was increased to 750°C for 1 min, all the perovskite structure peaks appeared along with a second phase peak at 2θ ~ 35.9°. No such second-

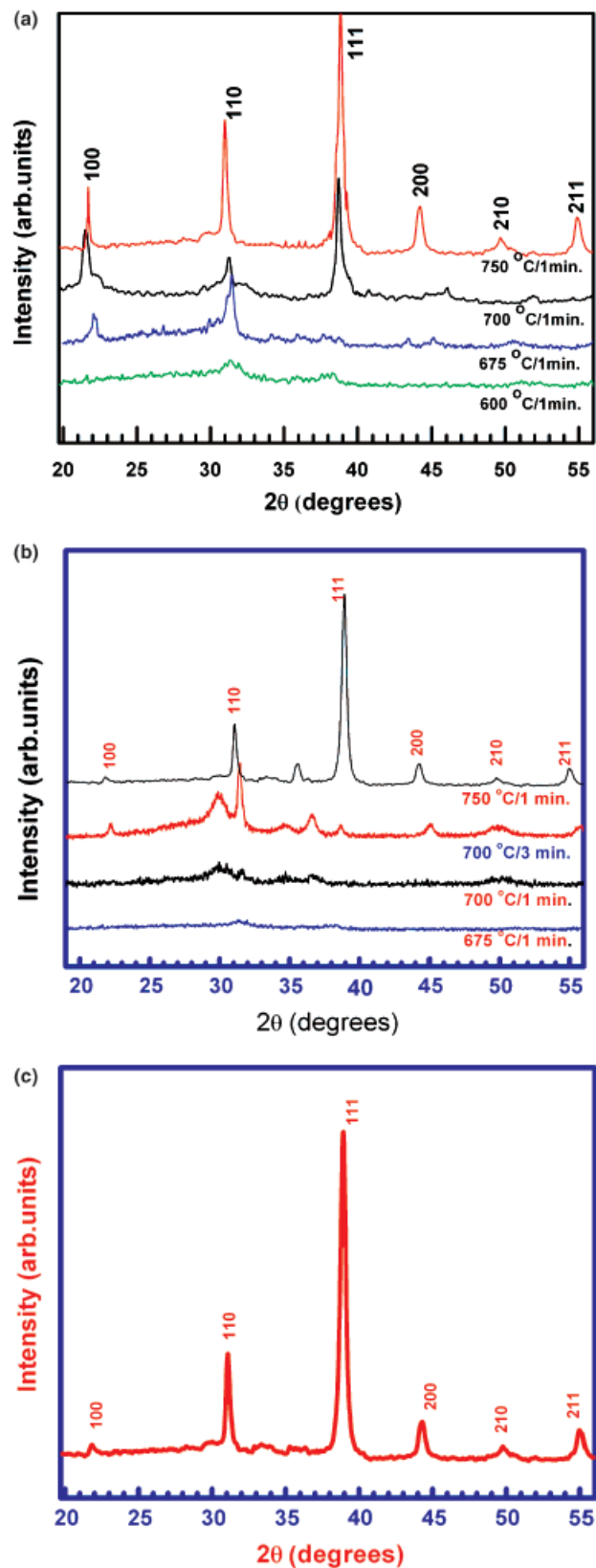


Fig. 6. X-ray diffraction of (a) LaNiO₃ and (b) $\text{Pb}(\text{Zr}_{0.52}\text{Ti}_{0.48})\text{O}_3$ (PZT) tubes microtubes as a function of annealing temperature and (c) PZT tubes deposited after three infiltrations of a LaNiO₃ buffer layers. These bilayers were annealed at 750°C for 1 min.

ary phase was noticed in the X-ray pattern of LaNiO₃/PZT bilayer tubes, suggesting that LaNiO₃ served as a barrier layer, preventing reaction between lead in PZT with the silicon matrix (Fig. 7(c)). This would be consistent with previous reports for flat films with LaNiO₃ buffer layers.²⁸

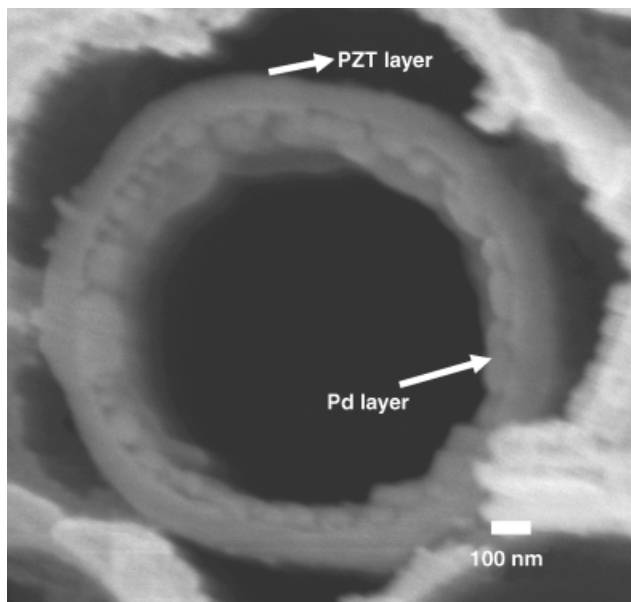


Fig. 7. Cross-sectional scanning electron microscopy image of a coaxial bi-layer $\text{Pb}(\text{Zr}_{0.52}\text{Ti}_{0.48})\text{O}_3$ (PZT)/Pd tube structure. The inner Pd layer has larger grains compared with the outer PZT layer.

It is interesting to note that the thermal budget required to crystallize the released tubes was higher than that required to process well-crystallized planar films.²⁹ Thus, a well-crystallized sol-gel-deposited planar PZT thin film on a LaNiO_3 -coated Si substrate was achieved at 700°C for 1 min using RTA. The difference in the crystallization temperatures between tubes and thin films could be a consequence of poor thermal contact between the released tubes and the underlying substrate.

Bright-field transmission electron microscope (TEM) images of the microstructures of PZT tubes are shown in Fig. 8. As can be seen, the microtubes are comprised of two different polycrystalline phases (Figs. 8(a) and 8(b)); the average grain size of the perovskite phase was estimated to be 100–150 nm, whereas the pyrochlore grains were approximately 5–10 nm in size. The majority of the tube, as seen in Fig. 8(a), is comprised of the large perovskite crystals, but the pyrochlore phase is still present in small amounts throughout the tube. The Moiré fringes observed in the high-resolution TEM (Fig. 8(c)) are a result of



Fig. 9. Selective electron diffraction pattern of $\text{Pb}(\text{Zr}_{0.52}\text{Ti}_{0.48})\text{O}_3$ (PZT) microtubes from the area in Fig. 8(c). The single crystalline pattern originates from the large single crystals of PZT, whereas the polycrystalline ring is from the smaller pyrochlore phase.

small pyrochlore grains overlapping the large perovskite crystallite. A selected area diffraction (SAD) pattern from the PZT tube in Fig. 8(c) is shown in Fig. 9. The single crystalline diffraction pattern corresponds to the perovskite structure of PZT, while the polycrystalline ring corresponds to the face-centered cubic (FCC) structure of the pyrochlore.

Previous research on preparation of high aspect ratio structures using a Si template utilized a procedure in which the amorphous ferroelectric was first annealed at high temperatures and then released from the template.^{18–20} However, the reaction between Si and PZT is detrimental to perovskite phase formation in PZT, as is shown in Fig. 10. The resulting degradation in phase purity will certainly affect the properties. In the present studies, second phase formation in PZT tubes prepared using Si templates could only be achieved by avoiding direct contact with the Si during heat treatments. LaNiO_3 served as an appropriate barrier for this purpose.

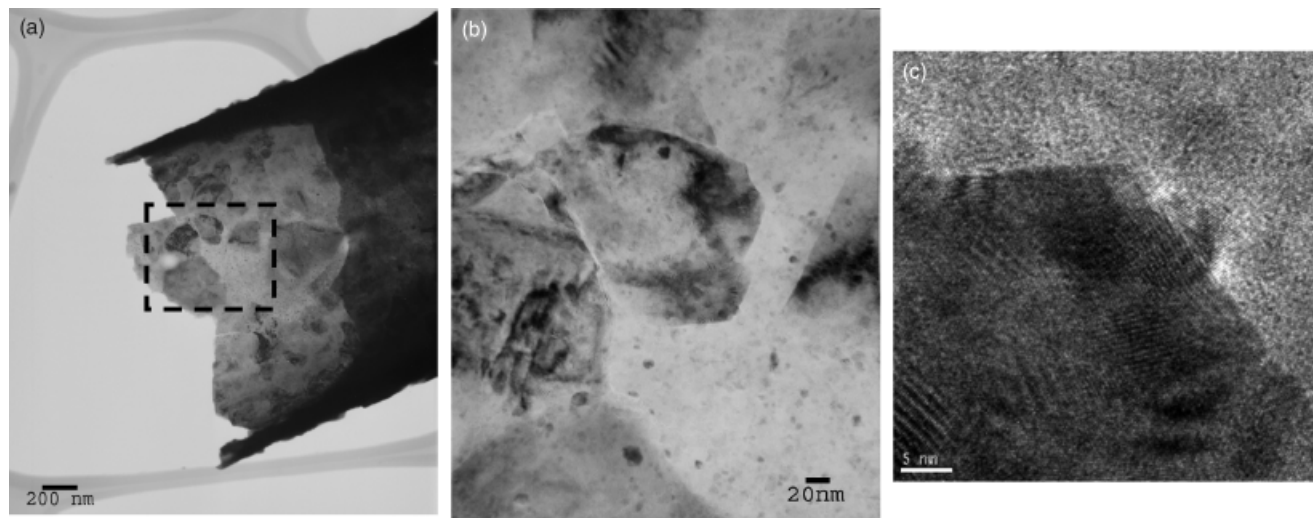


Fig. 8. Bright-field transmission electron microscopy (TEM) images of (a) a $\text{Pb}(\text{Zr}_{0.52}\text{Ti}_{0.48})\text{O}_3$ microtube and (b) a magnified view of the highlighted area in (a). These tubes were annealed at 750°C for 1 min after releasing from the silicon mold (c). High-resolution TEM image of the interface between a perovskite crystallite and an area of pyrochlore phase. The Moiré fringes in the image are a result of the small 5–10 nm pyrochlore crystals overlapping the large perovskite single crystals.

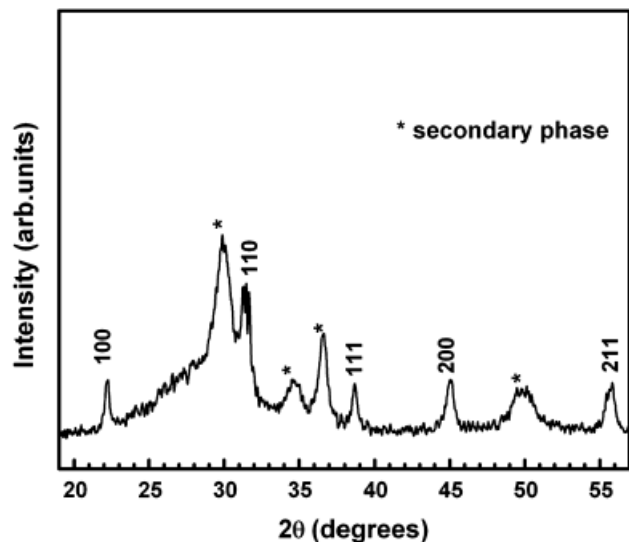


Fig. 10. X-ray diffraction pattern of $\text{Pb}(\text{Zr}_{0.52}\text{Ti}_{0.48})\text{O}_3$ tubes annealed in the silicon mold at 700°C for 1 min and released.

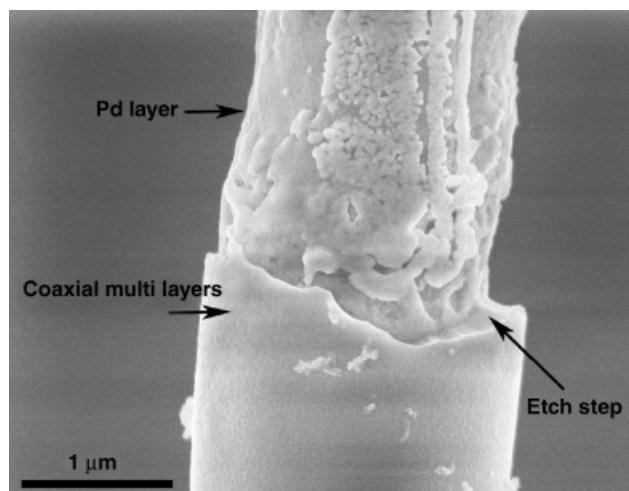


Fig. 11. Scanning electron microscopy image of a coaxial multilayer $\text{LaNiO}_3/\text{Pb}(\text{Zr}_{0.52}\text{Ti}_{0.48})\text{O}_3$ (PZT)/ LaNiO_3/Pd tube. The exposed inner Pd layer can be seen. The bumps on the tube are probably insoluble metal fluorides that develop when PZT is etched in buffered oxide etch.³⁰

Figure 11 shows an SEM image of $\text{LaNiO}_3/\text{PZT}/\text{LaNiO}_3/\text{Pd}$ concentric structures with an exposed inner Pd contact. For this purpose, following the optimal processing conditions for individual LaNiO_3 , PZT, and Pd layers, concentric multilayer $\text{LaNiO}_3/\text{PZT}/\text{LaNiO}_3/\text{Pd}$ microtubes were processed. Later, these tubes were partially released from the Si template using gas-phase etching. The released parts of the tubes were exposed to BOE solution for 5 min. to remove the oxide layers and expose the inner Pd layer.³⁰ Subsequently, the rest of the Si template was removed using gas-phase etching as described in earlier sections. It can be seen that in this way access to inner and outer electrodes can be achieved. A future paper will report on the electrical and electromechanical properties of these structures.

IV. Summary

In summary, the vacuum infiltration method for fabricating high aspect ratio ferroelectric $\text{Pb}(\text{Zr}_{0.52}\text{Ti}_{0.48})\text{O}_3$, LaNiO_3 , and Pd microtube structures using Si templates was described. The release of microtube structures from the silicon template before annealing reduced secondary phase formation in PZT micro-

tubes. A thin layer of LaNiO_3 served as a barrier layer between the PZT and the Si template for in-mold crystallization, minimizing the development of secondary phases in PZT tubes. Use of RIE, followed by a XeF_2 release, reduced surface damage to the tubes relative to release in KOH. The perovskite phase formation temperatures of these tubes were found to be significantly higher than those for planar thin films. In addition, the processing of coaxial multilayer tube structures, such as $\text{LaNiO}_3/\text{PZT}/\text{LaNiO}_3/\text{Pd}$, is described, along with a method to expose the inner and outer contacts.

References

- K. A. Klicker, J. V. Biggers, and R. E. Newnham, "Composites of PZT and Epoxy for Hydrostatic Transducer Applications," *J. Am. Ceram. Soc.*, **64**, 5–9 (1981).
- E. K. Akdogan, M. Allahverdi, and A. Safari, "Piezoelectric Composites for Sensor and Actuator Applications," *IEEE Trans. Ultrason. Ferroelectr. Frequency Control*, **52**, 746–75 (2005).
- J. E. Smay, J. Cesarano III, B. A. Tuttle, and J. A. Lewis, "Piezoelectric Properties of 3- X Periodic $\text{Pb}(\text{Zr}_x\text{Ti}_{1-x})\text{O}_3$ -Polymer Composites," *J. Appl. Phys.*, **92**, 6119–27 (2002).
- T. R. Gururaja, W. A. Schulze, L. E. Cross, R. E. Newnham, B. A. Auld, and Y. J. Wang, "Piezoelectric Composite Materials for Ultrasonic Transducer Applications. Part I: Resonant Modes of Vibration of PZT Rod-Polymer Composites," *IEEE Trans. Sonics Ultrason.*, **SU-32**, 481–98 (1985).
- S. Wang, J.-F. Li, K. Wakabayashi, M. Esashi, and R. Watanabe, "Lost Silicon Mold Process for PZT Microstructures," *Adv. Mater.*, **11**, 873–6 (1999).
- J. F. Scott, F. D. Morrison, M. Miyake, P. Zubko, X. J. Lou, V. M. Kugler, S. Rios, M. Zhang, T. Tatsuta, O. Tsuji, and T. J. Leadham, "Recent Materials Characterizations of [2D] and [3D] Thin Film Ferroelectric Structures," *J. Am. Ceram. Soc.*, **88**, 1691–701 (2005).
- S. S. N. Bharadwaja, D. J. Won, H. Fang, V. Gopalan, S. Trolier-McKinstry, N. Saldanha, and T. Mayer, "Processing and Properties of High Aspect Ratio Ferroelectric Structures"; pp. 189–91 in *14th IEEE International Symposium on Applications of Ferroelectrics-ISAF-04*, Edited by M. P. Yuhas. Montreal, Canada, 2004.
- G. A. Rossetti, L. E. Cross, and K. Kushida, "Stress-Induced Shift of the Curie-Point in Epitaxial PbTiO_3 Thin-Films," *Appl. Phys. Lett.*, **59**, 2524–6 (1991).
- N. A. Pertsev, A. G. Zembilgotov, and A. K. Tagantsev, "Effect of Mechanical Boundary Conditions on Phase Diagrams of Epitaxial Ferroelectric Thin Films," *Phys. Rev. Lett.*, **80**, 1988–91 (1998).
- S. K. Streiffer, C. B. Parker, A. E. Romanov, M. J. Lefevre, L. Zhao, J. S. Speck, W. Pompe, C. M. Foster, and G. R. Bai, "Domain Patterns in Epitaxial Rhombohedral Ferroelectric Films. I. Geometry and Experiments," *J. Appl. Phys.*, **83**, 2742–53 (1998).
- N. A. Pertsev, A. G. Zembilgotov, S. Hoffmann, R. Waser, and A. K. Tagantsev, "Ferroelectric Thin Films Grown on Tensile Substrates: Renormalization of the Curie-Weiss Law and Apparent Absence of Ferroelectricity," *J. Appl. Phys.*, **85**, 1698–701 (1999).
- F. Xu, S. Trolier-McKinstry, W. Ren, B. Xu, Z.-L. Xie, and K. J. Hemker, "Domain Wall Motion and its Contribution to the Dielectric and Piezoelectric Properties of Lead Zirconate Titanate Films," *J. Appl. Phys.*, **89**, 1336–48 (2001).
- A. Stanishevsky, B. Nagaraj, J. Melngailis, R. Ramesh, L. Khriachtchev, and E. McDaniel, "Radiation Damage and its Recovery in Focused Ion Beam Fabricated Ferroelectric Capacitors," *J. Appl. Phys.*, **92**, 3275–8 (2002).
- M. Alexe, C. Harnagea, and D. Hesse, "Non-conventional Micro- and Nanopatterning Techniques for Electroceramics," *J. Electroceram.*, **12**, 69–88 (2004).
- G. Suyal, E. Colla, R. Gysel, M. Cantoni, and N. Setter, "Piezoelectric Response and Polarization Switching in Small Anisotropic Perovskite Particles," *Nano Lett.*, **4** [7] 1339–42 (2004).
- J.-F. Liu, X.-L. Li, and Y.-D. Li, "Novel Synthesis of Polymorphous Nanocrystalline KNbO_3 by a Low Temperature Solution Method," *J. Nanosci. Nanotechnol.*, **2**, 617–9 (2002).
- J. J. Urban, J. E. Spanier, L. Ouyang, W. S. Yun, and H. Park, "Single-Crystalline Barium Titanate Nanowires," *Adv. Mater.*, **15**, 423–6 (2003).
- T. Aoki, S. Shimada, K. Kurihara, and M. Kuwabara, "Fabrication and Properties of PLZT Photonic Crystal Using a Sol-Gel Method"; pp. 69–72 in *The 11th US-Japan Seminar on Dielectric & Piezoelectric Ceramics*, September 9–12, 2003.
- K.-S. Chang, B. A. Hernandez, E. R. Fisher, and P. K. Dorhout, "Sol-Gel Template Synthesis and Characterization of PT, PZ, and PZT Nanotubes," *J. Korean Chem. Soc.*, **46**, 241–51 (2002).
- E. D. Mishina, N. E. Sherstyuk, V. I. Stadnuchyuk, K. A. Vorotilov, V. A. Vasil'ev, A. S. Sigov, O. M. Zhigalina, N. Ohta, and S. Nakabayashi, "Ferroelectrics Templated in Nanoporous Silicon Membranes," *Ferroelectrics*, **286**, 205–11 (2003).
- Y. Luo, I. Szafraniak, N. D. Zakharov, V. Nagarajan, M. Steinhart, R. B. Wehrspohn, J. H. Wendorff, R. Ramesh, and M. Alexe, "Nanoshell Tubes of Ferroelectric Lead Zirconate Titanate and Barium Titanate," *Appl. Phys. Lett.*, **83**, 440–2 (2003).
- F. D. Morrison, L. Ramsay, and J. F. Scott, "High Aspect Ratio Piezoelectric Strontium-Bismuth-Tantalate Nanotubes," *J. Phys. Condens. Matter*, **15**, L527–32, (2003).

²³R. A. Wolf and S. Trolier-McKinstry, "Temperature Dependence of the Piezoelectric Response in Lead Zirconate Titanate Films," *J. Appl. Phys.*, **95**, 1397–406 (2004).

²⁴M. Steinhart, Z. Jia, A. K. Schaper, R. B. Wehrspohn, U. Gösele, and J. H. Wendorff, "Palladium Nanotubes with Tailored Wall Morphologies," *Adv. Mater.*, **15**, 706–9 (2003).

²⁵Y. Ling, W. Ren, X.-Q. Wu, L.-Y. Zhang, and X. Yao, "Preparation and Properties of Conductive LaNiO₃ Thin Films by a Thermal Decomposition of Water-Based Solutions," *Thin Solid Films*, **311**, 128–32 (1997).

²⁶X.-J. Meng, J.-L. Sun, J. Yu, H.-J. Ye, S.-L. Guo, and J.-H. Chu, "Preparation of Highly (1 0 0)-Oriented Metallic LaNiO₃ on Si Substrates by a Modified Metalorganic Decomposition Technique," *Appl. Surf. Sci.*, **171**, 68–70 (2001).

²⁷G. R. Fox, S. Trolier-McKinstry, L. Casas, and S. B. Krupanidhi, "Pt/Ti/SiO₂/Si Substrates," *J. Mater. Res.*, **10**, 1508–15 (1995).

²⁸D. Bao, X. Yao, N. Wakiya, K. Shinozaki, and N. Mizutani, "Preparation of Conductive LaNiO₃ Film Electrodes by a Simple Chemical Solution Deposition Technique for Integrated Ferroelectric Thin Film Devices," *J. Phys. D: Appl. Phys.*, **36**, 1217–21 (2003).

²⁹S. Trolier-McKinstry, J. Chen, K. Vedam, and R. E. Newnham, "In Situ Annealing Studies of Sol-Gel Ferroelectric Thin Films by Spectroscopic Ellipsometry," *J. Am. Ceram. Soc.*, **78**, 1907–13 (1995).

³⁰L.-P. Wang, R. Wolf, Q. Zhou, S. Trolier-McKinstry, and R. J. Davis, "Wet-etch Patterning of Lead Zirconate Titanate (PZT) Thick Films for Microelectromechanical Systems (MEMS) Applications"; pp. EE5.39, in *Materials Research Society Symposium Proceedings*. Vol. 657, Boston, 2001. □